Capturing Time-Resolved Prescribed Fire Emissions with TEMPO Special Observations

Qindan Zhu[1,*], Tianjia Liu[2,*], Makoto Kelp[3,*]

[1]Smithsonian Astrophysical Observatory, Center for Astrophysics | Harvard & Smithsonian, Cambridge, MA 02138, USA
[2]Department of Geography, University of British Columbia, Vancouver, BC V6T 1Z2, Canada
[3]Department of Atmospheric Sciences, University of Utah, Salt Lake City, UT 84112, USA
[*]These authors contributed equally to this work

Key Points:

- We present the first TEMPO measurements and emission estimates of individual prescribed fires.
- We quantify emissions from prescribed burns that are too small and short-lived to be captured by current satellite systems.
- Derived emissions agree with top-down and bottom-up estimates, while resolving the evolution of emissions through each burn.

Corresponding author: Qindan Zhu, qindan.zhu@cfa.harvard.edu

Abstract

Prescribed fires are widely used for land management in the United States, but their emissions remain difficult to quantify due to their small spatial extent and short duration. We present here the first demonstration that high-resolution "special observations" from the TEMPO geostationary instrument resolve sub-hourly nitrogen dioxide (NO_2) column enhancements from individual prescribed fires in the southeastern US. These observations are able to detect local plumes and track their evolution at minute-to-hourly timescales, enabling top-down and time-resolved emission estimates. Across four case studies in Alabama, Florida, and Georgia during 2025–2026, TEMPO quantifies emissions from individual prescribed fire events that could not previously be time-resolved by existing low-Earth-orbit satellite systems (e.g., TROPOMI, VIIRS). These results demonstrate that geostationary observations can quantify emissions from small, short-lived prescribed fires, thus improving representation of these emissions in inventories used for fire management and downstream air quality applications.

Plain Language Summary

Land managers in the United States deliberately set small, controlled fires, known as prescribed burns, to clear excess vegetation and to lower the risk of future wildfires. Because each prescribed burn is small and lasts only a few hours, previous satellites struggled to measure how much they emit. Here, we use special high-frequency observations from TEMPO, a geostationary satellite over North America that provides column measurements of nitrogen dioxide (NO_2) pollution. We track the NO_2 released by four prescribed fires in Alabama, Florida, and Georgia and estimate their emissions throughout each burn. Our emission estimates agree well with independent ground-based inventories in three of the four cases. These results show that TEMPO can provide emission information of these prescribed burns that can improve smoke forecasts and support burn planning decisions.

1 Introduction

Land managers and policymakers in North America face the challenge of deciding how to deploy limited resources to protect communities from increasingly severe wildfires, especially in the wildland–urban interface. In response, federal and state agencies are seeking to expand the use of prescribed burning to reduce fuel loads and mitigate the socio-ecological and public health impacts of large wildfires. In the US, this includes a national investment of nearly $2 billion for hazardous-fuel reduction through prescribed burning and other treatments (H.R. 5376, 2022), proposed legislation to streamline burn planning (H.R. 471, 2025), a California plan to treat one million acres annually across the state (California Governor's Forest Management Task Force, 2021), and other related legislation (S. 3044, 2025; S.B. 762, 2021; H.B. 2733, 2018; S.B. 25-007, 2025; 19.20.5 NMAC, 2022). However, the potential to avert widespread smoke exposure from future wildfires is not typically taken into consideration in prescribed fire planning (Sutherland & Edwards, 2022). Prescribed fire itself produces smoke that harms public health and disproportionately affects specific WUI communities (Afrin & Garcia-Menendez, 2021; **?**; Stowell et al., 2025). Quantitative measurements of prescribed fire emissions in North America remain limited, which hinders efforts to evaluate the consequences of expanding its use.

Prescribed fire can reduce future risk of wildfire and smoke exposure, but direct measurements of its emissions remain limited. Indigenous fire stewardship across North America has long demonstrated the value of frequent, low-severity burning to maintain ecosystem function and reduce hazardous fuels (Kolden, 2019; Wu et al., 2023; Higuera-Mendieta & Burke, 2026). Prescribed burns generally produce less smoke and have a higher combustion efficiency on average than wildfires (Marsavin et al., 2023). Recent work also suggests that prescribed burning can reduce net smoke emissions by reducing the severity of subsequent wildfires and can reduce the severity of subsequent wildfire burns (Kelp et al., 2025; Higuera-Mendieta & Burke, 2026; Davis et al., 2024; Strabo et al., 2026). However, those longer-term benefits are difficult to evaluate without direct information on the magnitude and timing of emissions from the burns themselves. Prescribed fire remains an air pollution source with near-term smoke impacts that are incompletely quantified and with public health impacts that remain highly uncertain (**?**). There is a critical gap in our ability to directly quantify emissions from individual treatments and to link those emissions to their air quality consequences.

Fire emissions are typically estimated using approaches that combine burned area, fuel consumption, and emission factors (van der Werf et al., 2025), or inferred from satellite observations of fire intensity (i.e., fire radiative power; FRP) and aggregate combustion and emissions factors derived from limited laboratory and field studies (Li et al., 2022). Compared to wildfires, prescribed fires are generally small (100–1000 acres), less intense, and short-lived, lasting only hours. This limits their detectability by existing satellites due to coarse spatial resolution (e.g., GOES-R) and infrequent overpasses (e.g., MODIS, VIIRS, Landsat, Sentinel-2). Persistent cloud cover and thick haze or smog can further obscure fires from satellite detection. Consequently, many events are missed entirely or are only partially observed, introducing uncertainty in the magnitude, duration, and timing of emissions. While state and federal agencies collect prescribed fire and burn permit records, the quality, accessibility, and completeness of datasets may vary widely across jurisdictions (Call et al., 2025). Some emission estimates rely on model-based approaches with a limited direct empirical basis, such as using scaling factors to account for discrepancies between satellite-derived burned area and burn permit records (Maji et al., 2026).

The launch of the TEMPO satellite in 2023 provides a new opportunity to directly observe prescribed fire emissions. The TEMPO instrument is a geostationary imaging spectrometer that provides direct hourly observations of trace gases across North America (Zoogman et al., 2017). Since its launch, TEMPO has been shown to resolve the di-

urnal evolution of urban and background NO_2 columns (Fioletov et al., 2025), diagnose diurnal shifts in ozone production regimes across US cities (Jin et al., 2025), and detect and track large NO_2 enhancements within wildfire smoke plumes (Schollaert et al., 2025). In addition to its standard observing mode, TEMPO performs targeted "special observations" over selected regions through non-routine tasking, providing a rare opportunity to sample trace gas variability at up to 5-minute temporal resolution and 2.1×4.5 km^2 spatial resolution. This capability is well-suited to prescribed fires, which have small footprints and short durations that fall below the detection limits of coarse or infrequently-sampling sensors. TEMPO special observations therefore provide a previously unavailable opportunity to track plume evolution and quantify emissions from individual treatments.

In this study, we use TEMPO special observations of prescribed fires in the southeastern US along with coincident active fire detections, smoke products, and meteorological data to resolve NO_2 column enhancements from individual prescribed fire treatments. We derive emissions at sub-hourly timescales, with measurements as frequent as every 5 minutes, and apply this framework to four case studies during 2025–2026. These cases span a diverse range of burn sizes, from 722 to 10,063 acres, and atmospheric conditions, including weak to moderate winds and differing levels of detectability by existing satellite products. We compare the resulting time-resolved emissions with coincident low-earth orbit (LEO) satellite observations and bottom-up estimates based on burned area and emission factors. Our results demonstrate, for the first time, that TEMPO quantifies emissions from prescribed fires at the spatial and temporal scales at which they occur, providing a new observational constraint on the magnitude and timing of emissions that is unavailable from existing satellite systems.

2 Data and Methods

TEMPO special observations are used to retrieve tropospheric NO_2 columns at 5–15 minute intervals over each targeted region and to derive top-down emission estimates for four prescribed burning events. For each TEMPO scan, the NO_2 column field is rotated into the wind frame using NOAA High-Resolution Rapid Refresh (HRRR) (Dowell et al., 2022) meteorological winds and an exponentially modified Gaussian (EMG) is fit to the cross-wind integrated line density within a plume-aligned box (40 km upwind, 120 km downwind, $\pm$15 km crosswind) encompassing the NO_2 plume from each fire (Beirle et al., 2011). Only scans passing quality control criteria are retained for subsequent analysis. Comparisons are made with coincident active fire detections from VIIRS, MODIS, and GOES-East, digitized smoke plumes from NOAA's HMS smoke product, trace gas retrievals from TROPOMI, and bottom-up emission estimates calculated from burned area, fuel consumed, and emission factors.

2.1 Prescribed Fire Events

The four prescribed fire case studies are located in Geneva State Forest, Alabama (27 March 2025); Eglin Air Force Base and Blackwater River State Park ("Eglin–Blackwater"), Florida (28 March 2025); Chattahoochee–Oconee National Forest ("CONF"), Georgia (8 April 2026); and Fort Stewart, Georgia (12 April 2026). These fire events include one or more burn treatments that are digitized based on data from NASA FireSense airborne campaigns (Geneva), records from the USFS Southern Region Prescribed Burn Accomplishment Tracker (CONF), requested burn logs and burn unit maps (Fort Stewart), or satellite active fires and differenced Normalized Burn Ratio (dNBR, i.e., burn severity) derived from 30-m Harmonized Landsat and Sentinel-2 (HLS) imagery (Eglin–Blackwater) (Key & Benson, 2006; Ju et al., 2025). LEO active fire detections from MODIS (Terra, Aqua) and VIIRS (S-NPP, NOAA-20, NOAA-21) are retrieved from NASA's Fire Information for Resource Management System (FIRMS) (Davies et al., 2009). GOES-East

active fire detections and HLS imagery are retrieved from Google Earth Engine (Gorelick et al., 2017). Table 1 summarizes the four events.

Table 1. Summary of the four prescribed fire events.

Event	Date	Burn treatments (acres)	Total area (acres)	HMS smoke plumes	LEO fire detections[1]	HRRR wind speed[2] (m s^{-1})
Geneva State Forest, AL	27 Mar 2025	2 (177, 545)	722	None	MODIS/Terra (10:54)	2.7–3.6
Eglin–Blackwater, FL	28 Mar 2025	3 (4922, 1292, 3849)	10,063	1 light (GOES-East)	MODIS/Aqua (14:25), VIIRS/S-NPP (14:21), VIIRS/NOAA-20 (13:03, 14:43-14:44), VIIRS/NOAA-21 (13:56)	4.9–5.6
CONF, GA	8 Apr 2026	1 (1071)	1,071	1 medium, 1 light (GOES-West)	VIIRS/S-NPP (14:38), VIIRS/NOAA-20 (14:58), VIIRS/NOAA-21 (14:09)	4.4–4.6
Fort Stewart, GA	12 Apr 2026	1 (1148)	1,148	1 medium, 4 light (GOES-East/West)	VIIRS/NOAA-20 (13:43)	2.0–2.2

[1] LEO overpass times are given in local time (CDT or UTC-5 for AL and FL; EDT or UTC-4 for GA).
[2] Wind speeds are HRRR 900–1000 hPa averages over the source region.

2.2 Satellite Observations and Meteorological Data

We use Level-2 tropospheric NO_2 vertical column densities (VCDs) from the NASA TEMPO V04 retrieval products (TEMPO Science Team, 2024), focusing on special observation scans targeting prescribed fire events in the southeastern US during March–April 2025 and 2026. These TEMPO special observations provide measurements every 5–12 minutes at the native pixel resolution of approximately 2.1 km × 4.5 km at nadir (10 km^2). We retain only retrievals with the primary quality flag equal to zero.

For cross-satellite comparisons, we use the operational TROPOMI Level-2 tropospheric NO_2 product (Eskes et al., 2023) for the single Sentinel-5P overpass occurring within ±30 minutes of each TEMPO scan on the event day. We retain only TROPOMI retrievals with qa_value $\geq$ 0.5 and regrid the filtered swath onto the native TEMPO grid. Differences in the derived emissions (Q) between the two satellite products can therefore be attributed primarily to differences in the satellite retrievals themselves, providing an independent consistency check on the robustness of the TEMPO-based emission estimates.

We use GOES-16/19 ABI fire radiative power (FRP) observations at 5-minute temporal resolution to attribute observed plumes to specific burn treatments and to determine the active burning period for each event (Hall et al., 2019). For comparison against the TEMPO time series, we additionally use LEO active fire detections from the MODIS (Terra, Aqua; Giglio et al., 2016) and VIIRS (S-NPP, NOAA-20, NOAA-21; Schroeder et al., 2014) instruments retrieved from FIRMS, which provide an independent indicator of fire timing and location. Because these polar-orbiting sensors observe each fire at most once per overpass, they yield only a single snapshot of the burn, in contrast to the continuous sub-hourly sampling of TEMPO. In addition, we use smoke plume polygons from the NOAA Hazard Mapping System (HMS) Fire & Smoke product (T. Liu et al., 2024; NOAA Office of Satellite and Product Operations, 2026), which provide an separate qualitative indicator of smoke plume extent and transport. These smoke plumes include analyst-digitized polygons and qualitative classifications of smoke density as light, medium, or heavy.

For meteorological data, we use the hourly NOAA HRRR model at 3-km horizontal resolution (Dowell et al., 2022). For each TEMPO scan, we extract the u and v wind components averaged between 900 and 1000 hPa from the nearest HRRR time step and regrid them onto the native TEMPO Level-2 grid. The scalar wind speed and direction used to define the wind-aligned reference frame for each scan are calculated from the mean HRRR u and v values over all pixels within the cropped analysis window surrounding the burn centroid. Wind uncertainty is estimated as the standard error of the pixel-level wind speeds within the same analysis window.

2.3 Bottom-Up Emission Estimates

Our bottom-up emission estimates incorporate digitized fire perimeters, field-constrained fuel consumption, spatially explicit fuel loadings, and established emissions factors. First, to estimate burned area, we digitize prescribed burn perimeters for Geneva State Forest using NASA FireSense airborne infrared imagery (Majors & Pollard, 2025) with a spatial resolution of 1/3 arc-second (9 m), CONF using the USFS Southern Region Prescribed Burn Accomplishment Tracker, Fort Stewart using requested burn logs and burn unit maps, and Eglin–Blackwater using HLS-derived dNBR, guided by active fire detections aggregated by HMS. Second, we estimate fuel consumed using Consume fuel loadings mapped to 30-m LANDFIRE Fuel Characteristic Classification System Fuelbeds (FCCS) and three scenarios of low (25%), medium (50%), and high (75%) fuel consumption (FC) levels: FC25, FC50, and FC75 (Ryan & Opperman, 2013; Prichard et al., 2014). We apply a bias correction factor of 0.67 to FCCS fuel loadings based on an average ratio with FireSense pre-fire fuel measurements along six 22-m transects at Geneva State Forest (Robichaud et al., 2025). Finally, we apply NO_x emissions factors for southeastern US conifer forest based on Urbanski (2014) and Prichard et al. (2020).

2.4 Top-Down Emission Estimates

For each scan, the analysis window is a 200 km square crop centered on the event-specific source centroid, rotated into a wind-aligned coordinate system (ξ, η) with ξ along-wind and η cross-wind. Following Beirle et al. (2011), the EMG fitting domain is centered at $(\xi, \eta) = (0, 0)$ and spans $\xi \in [-40, +120]$ km and $\eta \in [-h, +h]$, where the cross-wind half-width defaults to $h = 15$ km and is expanded to 40 km for Eglin–Blackwater, whose broader source footprint requires a wider domain to capture the full cross-wind plume extent. The 120-km downwind extent corresponds to at least three plume e-folding lengths under typical HRRR wind speeds of 2–6 m s^{-1}, providing sufficient coverage to constrain the fits.

To identify scans containing detectable NO_2 plumes, we estimate a constant background B_{const} from a 30-km wide upwind sector outside the fitting domain and define a plume mask from pixels exceeding $B_{\mathrm{const}} + k\,\mathrm{MAD}$, where MAD is the median absolute deviation of NO_2 within the crop and $k_{\mathrm{MAD}} = 3$ by default (raised to 5 for larger, more diffuse plumes such as Eglin–Blackwater). We then apply a wind-alignment test to confirm that the detected plume orientation is consistent with the local wind direction.

For each detected plume, we compute the integrated line density $L(\xi)$ along the wind-aligned axis and fit it with an EMG following Beirle et al. (2011) and Laughner & Cohen (2019), characterized by the integrated source mass A, plume peak location μ, Gaussian width σ, first-order decay rate λ, and constant background B. The fitted A and λ yield the source emission rate as

$$Q[\mathrm{g\ NO\ s^{-1}}] = A\,\lambda\,v_{\mathrm{wind}} \times \frac{10^4}{N_A} \times r_{\mathrm{NO_x/NO_2}} \times M_{\mathrm{NO}}, \tag{1}$$

where v_{wind} is the HRRR-derived wind speed near the source, N_A is Avogadro's number, $r_{\mathrm{NO_x/NO_2}} = 1.32$ is the assumed $\mathrm{NO_x/NO_2}$ conversion ratio, and $M_{\mathrm{NO}} = 30$ g mol^{-1} converts to NO mass units. The corresponding effective lifetime is $\tau = 1000/(\lambda\, v_{\mathrm{wind}}\, 3600)$ h. Emissions are reported as NO rather than total $\mathrm{NO_x}$ to maintain consistency with the bottom-up inventory. Because these fires are short-lived, the EMG steady-state assumption holds in the near field, and we interpret τ as an effective lifetime that combines chemical loss and physical dilution.

We screen the EMG fits with four quality-control (QC) criteria, following thresholds adapted from previous EMG studies (Beirle et al., 2011; Laughner & Cohen, 2019): (1) coefficient of determination $R^2 \geq 0.5$; (2) peak position μ within the fitting domain; (3) Gaussian width $\sigma \in [\sigma_{\min}, \sigma_{\max}]$, with $\sigma_{\min} = 1$ km (relaxed to 0.5 km for CONF, whose compact 1,000-acre source produces physically narrower plumes) and event-specific $\sigma_{\max}$; and (4) lifetime $\tau \in [0.1, 6]$ h with $Q > 0$. The fractional uncertainty in Q is the quadrature sum of five independent terms, including the fit covariance of $A\lambda$, the wind-speed error σ_v/v (the standard error of HRRR wind speeds across the analysis window), the TEMPO Level-2 single-pixel retrieval uncertainty $s_{\mathrm{VCD}} = 0.25$, the background uncertainty $s_{\mathrm{bg}} = 0.10$, and the $\mathrm{NO_x/NO_2}$ ratio uncertainty $s_{\mathrm{ratio}} = 0.10$. For each event, the total NO emission is the median QC-passing Q multiplied by the GOES-defined active-window duration, taken as the elapsed time between the first and last detected scan.

3 Results and Discussion

TEMPO special observations resolve $\mathrm{NO_2}$ column enhancements from individual prescribed fires across multiple sites in the southeastern US. Figure 1 shows retrieved $\mathrm{NO_2}$ columns with distinct plumes aligned with burn treatment polygons identified from airborne observations and complementary satellite imagery capturing smoke plumes. These enhancements are distinguishable from background variability and persist over the duration of active burning. For example, at Geneva State Forest (Alabama), plumes are detected from two burns occurring in close succession (545 and 177 acres), demonstrating sensitivity to fire activity at spatial and temporal scales below the detection limits of the HMS smoke plume product (T. Liu et al., 2024). Similarly, at CONF (Georgia), a burn of 1,071 acres produces a well-defined $\mathrm{NO_2}$ column plume consistent with mapped burn area. At peak burning, $\mathrm{NO_2}$ vertical column density within the plume footprint is enhanced by 152% above background at Geneva State Forest and 133% above background at CONF, with mean enhancements over the active burn period of 74% and 33%, respectively. These observations together show that TEMPO detects and resolves emissions from individual prescribed fires across a range of treatment sizes and atmospheric conditions.

The high temporal resolution of TEMPO enables direct characterization of emission dynamics at sub-hourly timescales. As shown in Figure 2, we derive top-down $\mathrm{NO_x}$ emission estimates at each TEMPO observation time through the burn period, yielding 5 to 14 scans per event. Across four prescribed fire events spanning more than an order of magnitude in emissions, per-scan emission rates show rapid increases associated with active burning with median emission rates ranging from 270 g NO s^{-1} at the smaller CONF and Geneva State Forest fires to 2,860 g NO s^{-1} at Eglin–Blackwater. Within individual events, per-scan emission rates vary by roughly a factor of 2 to 3 over the burn (e.g., 220–750 g NO s^{-1} at Geneva State Forest), capturing event-specific evolution that includes both rapid buildup (e.g., Fort Stewart) and gradual decay (e.g., CONF) in $\mathrm{NO_2}$. At Fort Stewart, per-scan emissions rose by nearly two orders of magnitude, from 67 to 4,057 g NO s^{-1} within the first 20 minutes of detection before subsiding. Figure S1 shows the per-scan $\mathrm{NO_2}$ columns for every QC passing scan of the CONF fire on 8 April 2026. The $\mathrm{NO_2}$ column plume strengthens through the early afternoon, reaches a maximum roughly 1.3 hours after ignition, and then decays over the following hour, mirroring the evolution of the fitted emission rate Q. Throughout the burn, the plume core remains

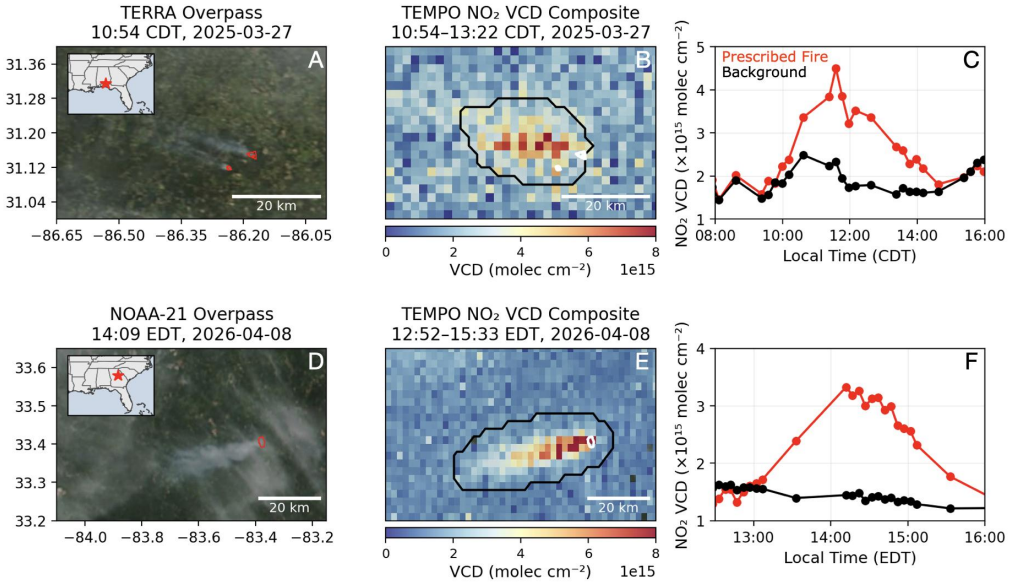

Figure 1. TEMPO NO_2 enhancements from individual prescribed fires. The top row shows Geneva State Forest, Alabama, on 27 March 2025, and the bottom row shows Chattahoochee–Oconee National Forest, Georgia, on 8 April 2026. Left panels (A, D) show true-color satellite imagery with prescribed burn perimeters outlined in red. Center panels (B, E) show TEMPO tropospheric NO_2 vertical column density (VCD) overlaid with the same prescribed burn perimeters in white. Black contours denote the smoke plume identified independently for each TEMPO scan using an HRRR wind-aware detection algorithm and outline the core region of persistent NO_2 enhancement. Right panels (C, F) show TEMPO NO_2 VCD time series averaged over pixels within the detected plume (red) and within a background region (black). Local times are CDT (UTC−5) for Alabama and EDT (UTC−4) for Georgia.

anchored near the source rather than advecting progressively downwind, which is consistent with the near-field steady-state assumption underlying the EMG retrieval (Beirle et al., 2011). Because the fires are short-lived, the inferred Q primarily reflects recent, near-source emissions, so the retrieval tracks a physical signal rather than a systematic downwind drift of the plume. In several cases, we detect emissions during periods when other satellite products report no fire activity or smoke. For instance, at Geneva State Forest and Fort Stewart, TEMPO captures sustained NO_2 column enhancements during intervals without active fire detections from VIIRS and MODIS, digitized smoke plumes from HMS, or NO_2 enhancements from TROPOMI. Polar-orbiting sensors capture at most a single scan of prescribed fires and only when the satellite overpass coincides with the active burning period (at 3.2 hours for the Eglin–Blackwater fires and 1.8 hours for the CONF fire after ignition). Across the four events, TEMPO provides 37 QC-passing retrievals, compared to only 2 coincident TROPOMI retrievals. Although emission estimates from coincident TROPOMI retrievals are broadly consistent with TEMPO within 50%, such overlaps are infrequent and TROPOMI does not capture the full temporal evolution of these events. As a result, only TEMPO resolves the sub-hourly structure of these short-lived emission pulses.

Compared to top-down estimates, bottom-up approaches target the overall magnitude of fire emissions, although some inventories approximate the sub-daily temporal structure using active fire observations (van der Werf et al., 2025; Li et al., 2022). The

bottom-up approach is sensitive to uncertainty in the components of its calculation: burned area or fire radiative energy, fuel consumption or scaling factors, and emissions factors. Due to broad land cover assumptions, variable satellite observing conditions, missing or false positive active fire detections, or coarse spatio-temporal resolution, estimates of each component can vary widely across fire events and inventories. In contrast, the top-down approach bypasses these components and directly observes and resolves the temporal structure of emissions. However, the top-down approach is likewise affected by satellite observing conditions, such as during highly cloudy and hazy periods.

We compare integrated TEMPO totals against the medium fuel-consumption scenario (FC50), with the FC25 and FC75 scenarios defining the bottom-up uncertainty envelope (Figure 2). Based on pre-fire and post-fire transect measurements at Geneva State Forest, the average fuel consumed by the 545-acre prescribed burn is 52%, which is close to the FC50 scenario (Robichaud et al., 2025). Our top-down emission estimates yield 2,668 kg NO [2,151–3,186] for Geneva, 45,439 kg NO for Eglin–Blackwater, 2,050 kg NO [1,390–2,709] for CONF, and 12,405 kg NO [5,292–19,518] for Fort Stewart. Three of the four events show moderate agreement with our bottom-up estimates, while the CONF event exhibits a large low bias. We attribute this discrepancy to intermittent cloudy conditions and heavy aerosol loading within the dense smoke plume, which introduces substantial uncertainty into the retrieved NO_2 column (S. Liu et al., 2024). In the four events, further differences could arise from assumptions in our fuel consumption estimates and high uncertainty in NO emission factors in the bottom-up estimates; the NO emissions factor for southeastern US conifer forests ranges from 1.7 (0.93) g kg^{-1} in Urbanski (2014) to 1.86 (1.8) g kg^{-1} in Prichard et al. (2020). As with other inventories, we did not incorporate the reported uncertainty for emission factors in our bottom-up estimates, though we note that this could help to further explain the observed differences between our top-down and bottom-up estimates. Finally, while we manually verified the area and location of the prescribed burns using agency records or high-resolution imagery for our bottom-up estimates, this is typically not the case for regional or global fire emissions inventories, which rely on moderate-resolution satellite observations of fires. Overall, the top-down and bottom-up estimates agree in total magnitude across the events when retrieval conditions are favorable, while TEMPO is able to resolve the dynamic timing and duration of emissions.

We note several limitations of our study. The top-down estimates depend on wind and plume geometry, as the EMG fitting requires a wind-aligned plume that is well separated from background variability. Fire events with weak or variable winds yield fewer QC-passing scans. The retrieval also assumes a fixed NO_x to NO_2 ratio (1.32), which introduces uncertainty under varying combustion and photochemical conditions. The CONF low bias further demonstrates that dense smoke with heavy aerosol loading degrade the NO_2 retrieval, suggesting that aerosol-corrected products is needed for the most intense burns, and that cloud cover corrections may be necessary in some cases. Finally, our analysis uses only four special observation event taskings, which limits the range of fire sizes and conditions sampled. We recommend future work to focus on expanding the number of tasked events and accounting for the aerosol correction in the NO_2 column retrievals for a better constraint of top-down NO_2 emission estimates.

4 Conclusions

TEMPO special observations offer a transformative capability for quantifying prescribed fire emissions by providing direct measurements of trace gases at the spatial and temporal scales at which these burns are conducted. This capability advances prescribed fire emissions from a quantity that is often largely inferred to one that can be observed directly at sub-hourly resolution. This information improves emission inventories and atmospheric modeling by constraining both the magnitude and timing of emissions from individual treatments, which in turn influence plume rise, transport, boundary-layer mix-

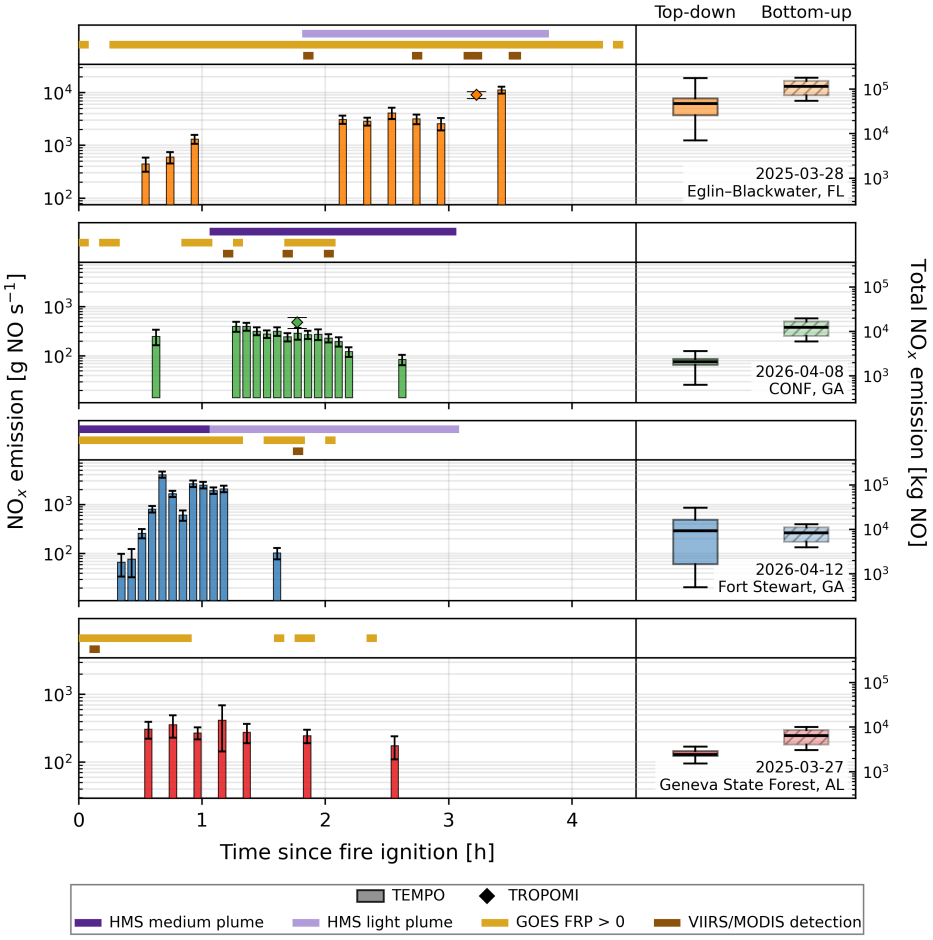

Figure 2. TEMPO resolves sub-hourly emissions from prescribed fire treatments and captures activity missed by other satellite products. NO_x emission rates for individual prescribed burn events are shown as a function of time since fire ignition with comparisons to bottom-up estimates. Each row corresponds to one event. Colored bars show the TEMPO per-scan EMG-fitted source rate, with 1σ error bars from the fit covariance, and diamonds show the corresponding TROPOMI estimate when a same-day overpass is available. The thin strip above each panel summarizes coincident observations from other products and, from top to bottom, shows HMS smoke polygons (light smoke in light lavender; medium smoke in dark purple), GOES-East FRP greater than zero (gold), and VIIRS/MODIS overpasses with at least one nominal-or-better fire detection near the source (brown). Box plots at right show the event-total NO_x emission (right axis, kg NO) from both top-down and bottom-up estimates. HMS here refers to analyst-digitized smoke polygons, which are distinct from the satellite active fire detections shown separately.

ing, chemical evolution, and downwind smoke exposure. The need for this ability is likely to grow as prescribed fire use expands in the western US (Kelp et al., 2025). In addition, TEMPO is highly synergistic with GOES to provide high-frequency observations of both active fires and trace gases (Li et al., 2022). Better quantification of emissions is needed to evaluate tradeoffs among short-term smoke impacts, long-term wildfire risk reduction, and ecosystem management objectives (Strabo et al., 2026). Direct observations of prescribed fire emissions will also support health-impact assessments by provid-

ing treatment-level estimates of when and where smoke is emitted (Qiu et al., 2025). They can also inform cost-benefit analyses and environmental justice evaluations by linking fire activity more explicitly to resulting exposure patterns (Kelp et al., 2023). Consequently, these measurements provide an observational basis for integrating prescribed fire into land management planning with substantially greater specificity than has previously been possible (Chung et al., 2025).

Open Research Section

TEMPO Level-2 NO_2 products are available from the NASA Atmospheric Science Data Center (TEMPO Science Team, 2024). The analysis code and intermediate datasets will be made available upon publication.

Conflict of Interest Statement

The authors have no conflicts of interest to disclose.

Acknowledgments

We thank the TEMPO science operations team for conducting the special observation scans. The work was conducted on the Smithsonian High Performance Cluster (SI/HPC), Smithsonian Institution (`https://doi.org/10.25572/SIHPC`). The analysis code and intermediate datasets will be made available upon publication.

References

19.20.5 NMAC. (2022). *Prescribed burn manager certification.* Retrieved from `https://www.srca.nm.gov/parts/title19/19.020.0005.html` (Administrative code)

Afrin, S., & Garcia-Menendez, F. (2021). Potential impacts of prescribed fire smoke on public health and socially vulnerable populations in a Southeastern U.S. state. *Science of the Total Environment*, *794*, 148712. doi: 10.1016/j.scitotenv.2021.148712

Beirle, S., Boersma, K. F., Platt, U., Lawrence, M. G., & Wagner, T. (2011). Megacity emissions and lifetimes of nitrogen oxides probed from space. *Science*, *333*(6050), 1737-1739. doi: 10.1126/science.1207824

California Governor's Forest Management Task Force. (2021). *California's wildfire and forest resilience action plan: Recommendations of the governor's forest management task force.* Retrieved from `https://wildfiretaskforce.org/wp-content/uploads/2022/04/californiawildfireandforestresilienceactionplan.pdf` (Report)

Call, A., Tomczyk, N., Withnall, K. A., Dappen, P. R., Heusinkveld, D., Mueller, S., ... Stevens-Rumann, C. S. (2025). A new geodatabase of fuel treatments across federal lands in the USA. *Scientific Data*, *12*, 1485. doi: 10.1038/s41597-025-05859-z

Chung, K. E., Liu, T., Kelp, M. M., Vohra, K., Skelly, D., Carroll, M. C., ... Mickley, L. J. (2025). Managing smoke risk from wildland fires: Northern california as a case study. *Environmental Science & Technology*, *59*(27), 13912-13923. doi: 10.1021/acs.est.5c01914

Davies, D. K., Ilavajhala, S., Wong, M. M., & Justice, C. O. (2009). Fire information for resource management system: Archiving and distributing MODIS active fire data. *IEEE Transactions on Geoscience and Remote Sensing*, *47*(1), 72-79. doi: 10.1109/TGRS.2008.2002076

Davis, K. T., Peeler, J., Fargione, J., Haugo, R. D., Metlen, K. L., Robles, M. D.,

& Woolley, T. (2024). Tamm review: A meta-analysis of thinning, prescribed fire, and wildfire effects on subsequent wildfire severity in conifer dominated forests of the western us. *Forest Ecology and Management*, *561*, 121885. doi: 10.1016/j.foreco.2024.121885

Dowell, D. C., Alexander, C. R., James, E. P., Weygandt, S. S., Benjamin, S. G., Manikin, G. S., ... Alcott, T. I. (2022). The high-resolution rapid refresh (HRRR): An hourly updating convection-allowing forecast model. part i: Motivation and system description. *Weather and Forecasting*, *37*(8), 1371-1395. doi: 10.1175/WAF-D-21-0151.1

Eskes, H., van Geffen, J., Boersma, F., Eichmann, K.-U., Apituley, A., Pedergnana, M., ... Loyola, D. (2023). *Sentinel-5 precursor/TROPOMI level 2 product user manual nitrogen dioxide* (Tech. Rep. No. S5P-KNMI-L2-0021-MA). Royal Netherlands Meteorological Institute (KNMI). Retrieved from `https://sentinels.copernicus.eu/documents/247904/2474726/Sentinel-5P-Level-2-Product-User-Manual-Nitrogen-Dioxide.pdf`

Fioletov, V., Griffin, D., McLinden, C. A., Zhao, X., Nowlan, C., & Abad, G. G. (2025). Diurnal variations in background and urban NO2 estimated from TEMPO. *Geophysical Research Letters*, *52*(21), e2025GL117360. doi: 10.1029/2025GL117360

Giglio, L., Schroeder, W., & Justice, C. O. (2016). The collection 6 MODIS active fire detection algorithm and fire products. *Remote Sensing of Environment*, *178*, 31-41. doi: 10.1016/j.rse.2016.02.054

Gorelick, N., Hancher, M., Dixon, M., Ilyushchenko, S., Thau, D., & Moore, R. (2017). Google Earth Engine: Planetary-scale geospatial analysis for everyone. *Remote Sensing of Environment*, *202*, 18-27. doi: 10.1016/j.rse.2017.06.031

Hall, J., Zhang, R., Schroeder, W., Huang, C., & Giglio, L. (2019). Validation of GOES-16 ABI and MSG SEVIRI active fire products. *International Journal of Applied Earth Observation and Geoinformation*, *83*, 101928. doi: 10.1016/j.jag.2019.101928

H.B. 2733. (2018). *Establishing a prescribed burn certification program at the department of natural resources.* 65th Washington Legislature, 2018 Regular Session. Retrieved from `https://lawfilesext.leg.wa.gov/Biennium/2017-18/Pdf/Bills/House%20Bills/2733.pdf` (Legislation)

Higuera-Mendieta, I., & Burke, M. (2026). The air pollution benefits of low-severity fire. *Science*, *392*(6803), eaea2490. doi: 10.1126/science.aea2490

H.R. 471. (2025). *Fix our forests act.* 119th Congress (2025–2026). Retrieved from `https://www.congress.gov/bill/119th-congress/house-bill/471` (Legislation)

H.R. 5376. (2022). *Inflation reduction act of 2022.* 117th Congress (2021–2022). Retrieved from `https://www.congress.gov/bill/117th-congress/house-bill/5376` (Legislation)

Jin, X., Yang, Y., Gonzalez Abad, G., Nowlan, C. R., & Liu, X. (2025). Observing the diurnal variations of ozone–NOx–VOC chemistry over the U.S. from the geostationary TEMPO instrument. *Geophysical Research Letters*, *52*(14), e2025GL116394. doi: 10.1029/2025GL116394

Ju, J., Zhou, Q., Freitag, B., Roy, D. P., Zhang, H. K., Sridhar, M., ... Neigh, C. S. (2025). The Harmonized Landsat and Sentinel-2 version 2.0 surface reflectance dataset. *Remote Sensing of Environment*, *324*, 114723. doi: 10.1016/j.rse.2025.114723

Kelp, M. M., Burke, M., Qiu, M., Higuera-Mendieta, I., Liu, T., & Diffenbaugh, N. S. (2025). Effect of recent prescribed burning and land management on wildfire burn severity and smoke emissions in the western united states. *AGU Advances*, *6*(3), e2025AV001682. doi: 10.1029/2025AV001682

Kelp, M. M., Carroll, M. C., Liu, T., Yantosca, R. M., Hockenberry, H. E., & Mick-

ley, L. J. (2023). Prescribed burns as a tool to mitigate future wildfire smoke exposure: Lessons for states and rural environmental justice communities. *Earth's Future*, *11*(6), e2022EF003468. doi: 10.1029/2022EF003468

Key, C. H., & Benson, N. C. (2006). *Landscape Assessment (LA). In: Lutes, Duncan C.; Keane, Robert E.; Caratti, John F.; Key, Carl H.; Benson, Nathan C.; Sutherland, Steve; Gangi, Larry J. 2006. FIREMON: Fire effects monitoring and inventory system* (Tech. Rep.). USDA Forest Service. Retrieved from `https://www.fs.fed.us/rm/pubs/rmrs_gtr164/rmrs_gtr164_13_land_assess.pdf`

Kolden, C. A. (2019). We're not doing enough prescribed fire in the western united states to mitigate wildfire risk. *Fire*, *2*, 30. doi: 10.3390/fire2020030

Laughner, J. L., & Cohen, R. C. (2019). Direct observation of changing NOx lifetime in north american cities [doi: 10.1126/science.aax6832]. *Science*, *366*(6466), 723-727. doi: 10.1126/science.aax6832

Li, F., Zhang, X., Kondragunta, S., Lu, X., Csiszar, I., & Schmidt, C. C. (2022). Hourly biomass burning emissions product from blended geostationary and polar-orbiting satellites for air quality forecasting applications. *Remote Sensing of Environment*, *281*, 113237. doi: 10.1016/j.rse.2022.113237

Liu, S., Valks, P., Curci, G., Chen, Y., Shu, L., Jin, J., ... Zhu, L. (2024). Satellite NO2 retrieval complicated by aerosol composition over global urban agglomerations: Seasonal variations and long-term trends (2001–2018) [doi: 10.1021/acs.est.3c02111]. *Environmental Science & Technology*, *58*(18), 7891-7903. doi: 10.1021/acs.est.3c02111

Liu, T., Panday, F. M., Caine, M. C., Kelp, M., Pendergrass, D. C., Mickley, L. J., ... James, E. P. (2024). Is the smoke aloft? caveats regarding the use of the hazard mapping system (HMS) smoke product as a proxy for surface smoke presence across the united states. *International Journal of Wildland Fire*, *33*. doi: 10.1071/WF23148

Maji, K. J., Li, Z., Hu, Y., Stowell, J. D., Milando, C. W., Vaidyanathan, A., ... Odman, M. T. (2026). Impact of prescribed fire emissions on ambient PM2.5 and its components in the southeastern US [doi: 10.1021/acsenvironau.6c00072]. *ACS Environmental Au*, *6*(3), 523-538. doi: 10.1021/acsenvironau.6c00072

Majors, L., & Pollard, C. (2025). *Nasa firesense 2025 tacfi-rs data.* (Accessed: 2026-04-18)

Marsavin, A., van Gageldonk, R., Bernays, N., May, N. W., Jaffe, D. A., & Fry, J. L. (2023). Optical properties of biomass burning aerosol during the 2021 Oregon fire season: comparison between wild and prescribed fires. *Environmental Science: Atmospheres*, *3*(3), 608-626. doi: 10.1039/d2ea00118g

NOAA Office of Satellite and Product Operations. (2026). *Hazard mapping system fire and smoke product.* Retrieved from `https://www.ospo.noaa.gov/Products/land/hms.html`

Prichard, S. J., Karau, E. C., Ottmar, R. D., Kennedy, M. C., Cronan, J. B., Wright, C. S., & Keane, R. E. (2014). Evaluation of the CONSUME and FOFEM fuel consumption models in pine and mixed hardwood forests of the eastern United States. *Canadian Journal of Forest Research*, *44*(7), 784–795. doi: 10.1139/cjfr-2013-0499

Prichard, S. J., O'Neill, S. M., Eagle, P., Andreu, A. G., Drye, B., Dubowy, J., ... Strand, T. M. (2020). Wildland fire emission factors in north america: synthesis of existing data, measurement needs and management applications. *International Journal of Wildland Fire*, *29*(2), 132-147. doi: 10.1071/WF19066

Qiu, M., Li, J., Gould, C. F., Jing, R., Kelp, M., Childs, M. L., ... Burke, M. (2025). Wildfire smoke exposure and mortality burden in the USA under climate change. *Nature*, *647*, 935-943. doi: 10.1038/s41586-025-09611-w

Robichaud, P., Miller, M., & Budd, S. (2025). *Nasa firesense geneva state forest burn ground fuel, moisture data and postfire assessment.* (Accessed: 2026-04-18)

Ryan, K. C., & Opperman, T. S. (2013). Landfire – a national vegetation/fuels data base for use in fuels treatment, restoration, and suppression planning. *Forest Ecology and Management*, *294*, 208–216. Retrieved from 10.1016/j.foreco.2012.11.003 doi: 10.1016/j.foreco.2012.11.003

S. 3044. (2025). *Wildfire emissions prevention act of 2025.* 119th Congress (2025–2026). Retrieved from https://www.congress.gov/bill/119th-congress/senate-bill/3044/all-info (Legislation)

S.B. 25-007. (2025). *Increase prescribed burns.* 75th Colorado General Assembly, 2025 Regular Session. Retrieved from https://leg.colorado.gov/bills/sb25-007 (Legislation)

S.B. 762. (2021). *Oregon senate bill 762.* 81st Oregon Legislative Assembly, 2021 Regular Session. Retrieved from https://olis.oregonlegislature.gov/liz/2021R1/Measures/Overview/SB762 (Legislation)

Schollaert, C. L., Connolly, R., Cushing, L., Jerrett, M., Liu, T., & Marlier, M. (2025). Air quality impacts of the january 2025 los angeles wildfires: Insights from public data sources. *Environmental Science & Technology Letters*, *12*, 911-917. doi: 10.1021/acs.estlett.5c00486

Schroeder, W., Oliva, P., Giglio, L., & Csiszar, I. A. (2014). The new VIIRS 375 m active fire detection data product: Algorithm description and initial assessment. *Remote Sensing of Environment*, *143*, 85-96. doi: 10.1016/j.rse.2013.12.008

Stowell, J. D., Maji, K. J., Li, Z., Hu, Y., Vaidyanathan, A., Milando, C., ... Wellenius, G. A. (2025). Associations between PM2.5 from prescribed burning and emergency department visits in 11 Southeastern US states. *Environment International*, *203*, 109770. doi: 10.1016/j.envint.2025.109770

Strabo, F., Bryan, C., & Reimer, M. N. (2026). Wildfire damages and the cost-effective role of forest fuel treatments [doi: 10.1126/science.aea6463]. *Science*, *392*(6798), 629-635. Retrieved from 10.1126/science.aea6463 doi: 10.1126/science.aea6463

Sutherland, S., & Edwards, E. (2022). *Does environmental review worsen the wildfire crisis? how environmental analysis delays fuel treatment projects* (PERC Policy Brief). Property and Environment Research Center (PERC). Retrieved from https://hdl.handle.net/10161/25599

TEMPO Science Team. (2024). *TEMPO tropospheric NO2 total and tropospheric column level 2 V04.* NASA Atmospheric Science Data Center (ASDC). doi: 10.5067/IS-40e/TEMPO/NO2_L2.004

Urbanski, S. (2014). Wildland fire emissions, carbon, and climate: Emission factors. *Forest Ecology and Management*, *317*, 51-60. doi: 10.1016/j.foreco.2013.05.045

van der Werf, G. R., Randerson, J. T., van Wees, D., Chen, Y., Giglio, L., Hall, J., ... Morton, D. C. (2025). Landscape fire emissions from the 5th version of the global fire emissions database (GFED5). *Scientific Data*, *12*(1), 1870. Retrieved from 10.1038/s41597-025-06127-w doi: 10.1038/s41597-025-06127-w

Wu, X., Sverdrup, E., Mastrandrea, M. D., Wara, M. W., & Wager, S. (2023). Low-intensity fires mitigate the risk of high-intensity wildfires in california's forests. *Science Advances*, *9*, eadi4123. doi: 10.1126/sciadv.adi4123

Zoogman, P., Liu, X., Suleiman, R. M., Pennington, W. F., Flittner, D. E., Al-Saadi, J. A., ... Chance, K. (2017). Tropospheric emissions: Monitoring of pollution (TEMPO). *Journal of Quantitative Spectroscopy and Radiative Transfer*, *186*, 17-39. doi: 10.1016/j.jqsrt.2016.05.008

Supporting Information for "Capturing Time-Resolved Prescribed Fire Emissions with TEMPO Special Observations"

Qindan Zhu[1,*], Tianjia Liu[2,*], Makoto Kelp[3,*]

[1]Smithsonian Astrophysical Observatory, Center for Astrophysics | Harvard & Smithsonian, Cambridge, MA 02138, USA
[2]Department of Geography, University of British Columbia, Vancouver, BC V6T 1Z2, Canada
[3]Department of Atmospheric Sciences, University of Utah, Salt Lake City, UT 84112, USA

[*]These authors contributed equally to this work

Contents of this file

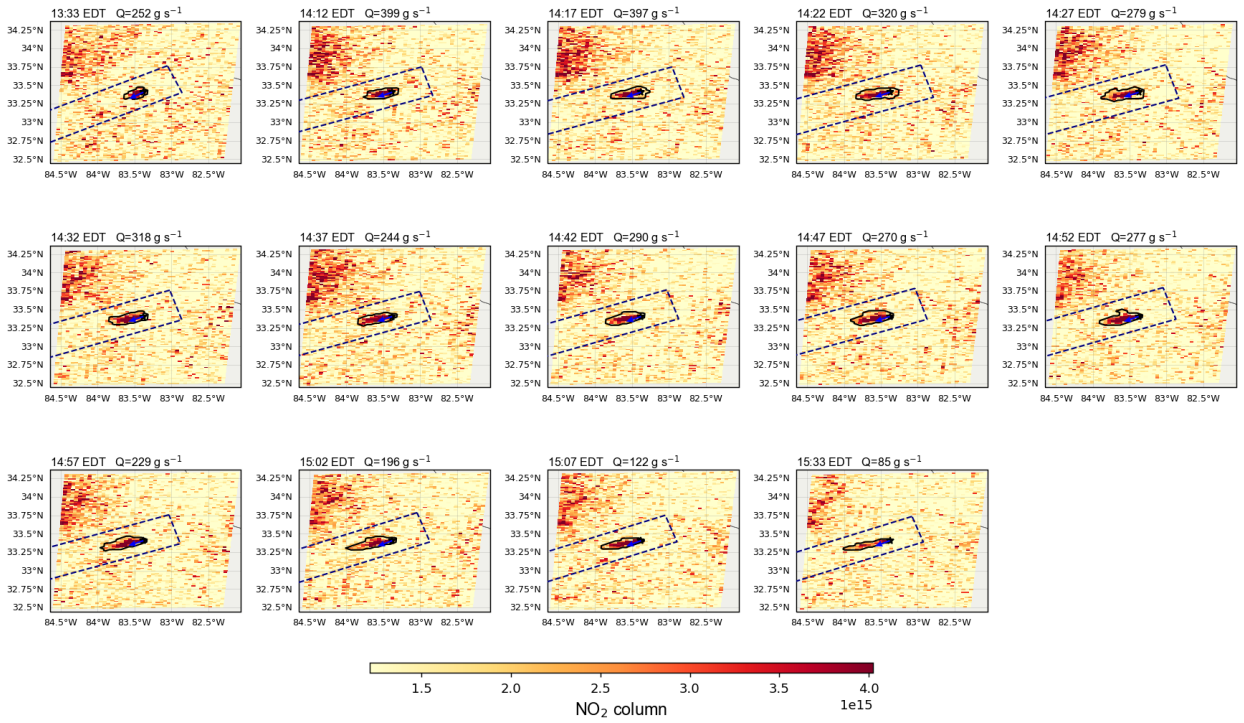

Figure S1: 14 QC-passed scans of TEMPO NO_2 column for the CONF, Georgia prescribed fire on 8 April 2026 (14 quality-control-passing scans). Each panel shows the NO_2 column in time order, with the wind-aligned EMG fitting box (navy dashed), the independently detected plume contour (black), the source location (star), and the near-source HRRR wind direction (blue arrow). Panel titles give the local time (EDT) and the fitted emission rate Q (g NO s^{-1}).